THE PENNSYLVANIA STATE UNIVERSITY
SCHREYER HONORS COLLEGE

DEPARTMENT OF CHEMISTRY

DIRECT POWDER SYNTHESIS OF MOLYBDENUM ALUMINUM BORIDE

ZACHARY METZGER
SPRING 2020

A thesis
submitted in partial fulfillment
of the requirements
for a baccalaureate degree
in Chemical Engineering
with honors in Area of Honors Chemistry

Reviewed and approved* by the following:

Raymond E. Schaak
Professor of Chemistry
Thesis Supervisor

Raymond L. Funk
Professor of Chemistry
Honors Adviser

* Signatures are on file in the Schreyer Honors College.

ABSTRACT

The synthesis, evaluation, and characterization of ternary borides were investigated as catalysts for the hydrogen-evolution reaction (HER) as well as for the formation of new 2D materials. MoAlB was targeted for these experiments due to its inherent layered structure and previous knowledge that bulk MoB is a highly active HER catalyst.[1,2,3,4] A new synthetic approach to directly form a powder of MoAlB, which is typically synthesized as single crystals, was also developed and optimized. Phase purity of both single crystal and powder forms was analyzed by X-ray diffraction. MoAlB was investigated in its single crystal and powder forms to test for electrocatalytic HER activity under acidic conditions.

TABLE OF CONTENTS

LIST OF FIGURES

Acknowledgments

I would like to extend a warm thank you to Dr. Raymond Schaak for offering me a position in his admirable research lab. He has helped me through college starting from when I took his second level general chemistry class as a freshman. At this point, he decided that he would invest not only his time, but the time of everyone in his research lab to help further my education outside the normal classroom environment. For that I am especially thankful for everyone in the research lab as well.

A special thank you to Lucas Alameda who has been there since the first day I walked into this research lab, a novice, but excited to learn. He took me on during one of the most high-pressure times in his graduate school career, and for that, I am forever thankful. He has brought me from an inexperienced lab-hand to a true expert in our field. I have relied on him from day one over these past three years and wish him the best in his future endeavors.

I would also like to extend my utmost thanks to my family. They have pushed me through college helping me at every step of the way. I always had the great pleasure of following my older sisters' footsteps in high school, and even in college, but now I know this was all so I could forge my own path towards a career. Lastly to my parents, who without them, I probably would not have been able to do research for two summers or even go to college comfortably. Thank you to everyone who has helped me get to where I am today.

Chapter 1:

Introduction

1.1 Introduction

As the world progresses towards a faster paced lifestyle that consumes energy at increasing volumes year after year, a critical need arises for a way to meet that demand.[5] The fuel of the future must be sustainable, highly efficient, low cost, and environmentally friendly. Hydrogen gas has been targeted as a clean energy source because upon combustion, it produces water vapor, contrasting its hydrocarbon counterparts that produce carbon dioxide, carbon monoxide, and various other poisonous and/or greenhouse gases.[5] This brings about the problem of how to cleanly obtain hydrogen gas. In the past, hydrogen gas has been produced in a few ways such as a by-product in crude oil processing; however, the hydrogen produced in this process is reliant on a non-renewable energy source and is usually used up later in the process eliminating it as a viable option.[6] The best alternative to this would be to identify a heterogenous hydrogen evolution reaction (HER) catalyst that can abstract hydrogen gas by water electrolysis.

1.2 Hydrogen Evolution Reaction (HER)

The hydrogen evolution reaction is proposed to reliably produce hydrogen via water electrolysis; however, the historically best catalysts for this reaction are

highly expensive and rare metals such as platinum, iridium, and palladium.[7] The ideal candidate is a catalyst that is earth-abundant, highly active for HER, and simple and inexpensive to produce. Many attempts have been successful in synthesizing catalysts that can mostly fit this profile, such as Ni_2P and CoP. For example, Ni_2P nanoparticles exhibited the best activity for HER within an earth-abundant system at the time of its publication.[8,9] This was a giant leap towards finding a catalyst for the HER that did not contain any non-earth abundant elements such as platinum or iridium. The use of the nanoparticle morphology does provide a much higher surface area than that of its bulk counterpart, but there are atoms that reside beneath the surface of the particle that do not react with the external environment. The ideal catalyst would minimize catalytically inactive core atoms and maximize catalytically active surface atoms. Two-dimensional (2D) materials may be able to meet this need based on the potential for them to have a much higher surface atom to total atom ratio.

1.3 Investigation of 2D Materials Derived from 3D Counterparts

The discovery of graphene in 2004 led to the increased interest in 2D materials as a research focus.[10] This discovery sparked a new section of research looking at the intrinsic properties of three-dimensional (3D) versus 2D materials such as the high strength of the material as well as its electronic properties in its 2D form.[11,12] A similar discovery was made in the HER catalyst field when MoS_2 was found to have no or minimal catalytic activity when it was in its bulk 3D form.

However, when it was modified to exist in its 2D form, it became active for HER. This discovery and others like it spiked an interest in the 2D community and motivates the question of what other properties of materials were unique to their 2D forms.

Since the discovery of graphene, the exploration of 2D materials has been in the forefront of many scientists' minds. Finding other materials that can be chemically or physically modified to form 2D materials was a key point of interest. A very interesting sub-group of 2D materials that have recently been discovered are MXenes, the 2D derivative of MAX phases.[13] MAX phases are bulk, layered solids that contain carbon or nitrogen and have the formula $M_{n+1}AX_n$ (MAX), where n=1 to 3 and 5.[14] These materials usually contain an early transition metal (M), a metalloid like Al or Si (A), and carbon or nitrogen (X).[15] These materials have been shown to be capable of having their structure delaminated to form 2D analogues (MXenes).[16] This delamination is caused by chemically etching the A element from the structure to leave 2D layers that are bonded in plane and made up of the MX elements, thus the designation MXenes – 2D "ene" nanosheets derived from bulk MAX phases. Figure 1, depicts the etching of the Al layer from the MAX phase structure to form a MXene.[15]

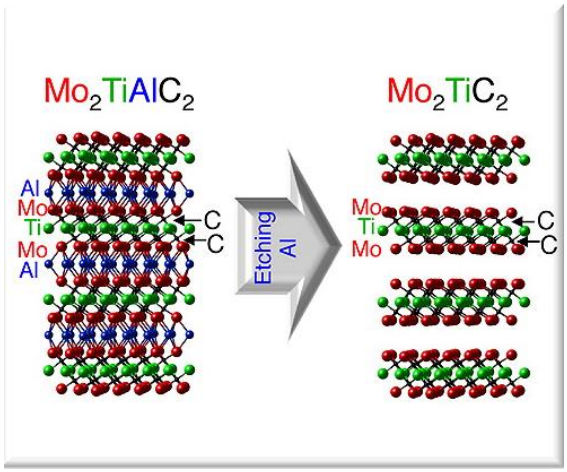

Figure 1: Structural comparison between MAX Phases (left) and a MXene (right). Adapted with permission from Babak Anasori, Yu Xie, Majid Beidaghi, Jun Lu, Brian C. Hosler, Lars Hultman, Paul R. C. Kent, Yury Gogotsi, and Michel W. Barsoum, *ACS Nano* 2015 *9* (10), 9507-9516. DOI: 10.1021/acsnano.5b03591. Copyright 2015 American Chemical Society.[21]

MXenes have been successfully applied to various energy storage applications such as Li-ion based energy storage technology or HER catalysis for water splitting, solar cells, and fuel cells.[17,18] However, their promising structure is currently limited in composition to early transition metal carbides and nitrides within the $M_{n+1}AX_n$ formula. There is a strong desire to maintain the useful structural features of MXenes while expanding them in composition beyond carbides and nitrides.

1.4 MAB Phases as Potential Avenues to Mimic MXenes

MAB phases are heterolayered metal borides that are gaining popularity due to their structural similarity to MAX phases. MAB phases exhibit interesting magnetocaloric effects and have the potential to form 2D “MBene” materials via etching the A element, in analogy to MAX phases forming MXenes. MAB phases

adopt several structure types including MAlB (M = Mo and W), M_2AlB_2 (M = Fe, Mn, Cr), M_3AlB_4, and M_4AlB_6 (M = Cr).[19] The most commonly studied phases are MoAlB and Fe_2AlB_2, due to a combination of their synthetic accessibility and the attractive properties exhibited by these two phases. MAB phases are a group of materials that were discovered by Jeitschko in the 1960's.[20] However, as a material class, they have received little attention relative to MAX phases due to the narrower compositional range of MAB phases and the general synthetic challenges related to metal borides relative the MAX phase carbides and nitrides.

MAB phases have a unique structural feature that distinguishes them from MAX phases and is a key factor for their 2D properties and potential catalytic activity. The synthetically accessible MAB phases, if fully etched to form a 2D material, would only have surface metal atoms while most MAX phases would have internal metal atoms not available for catalysis, as seen in Figure 2. For example, Mo_2TiAlC_2 forms Mo_2TiC_2 sheets (with buried titanium) upon etching Al, while MoAlB would form MoB sheets. The discovery of a MBene (a boride analog of a MXene) may lead to the discovery of a new 2D material with maximal surface area, high catalytic activity, and earth-abundant elements that is well suited for HER catalysis.

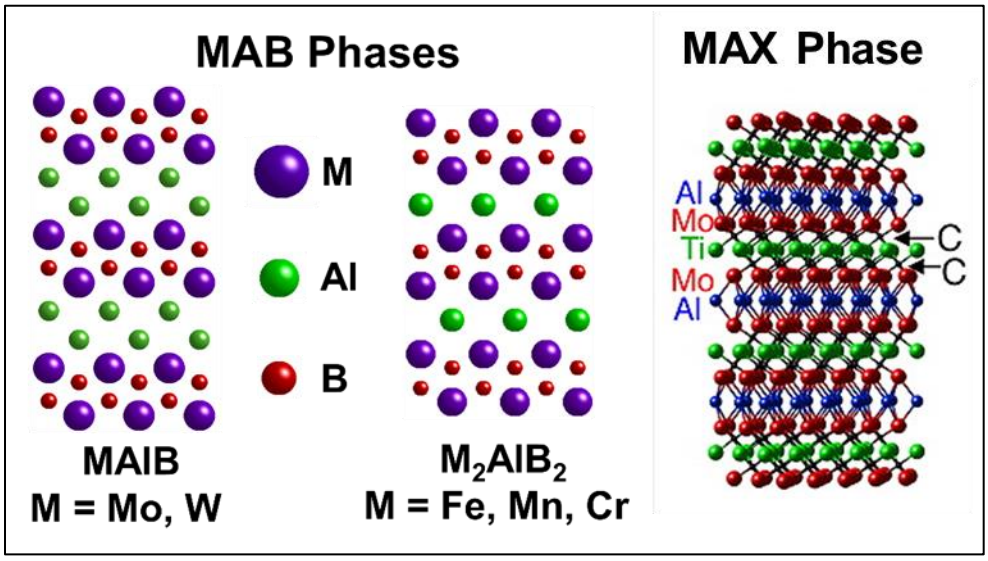

Figure 2: Structural comparison between MAB Phases (left) and a MAX phase (right). Adapted with permission from Babak Anasori, Yu Xie, Majid Beidaghi, Jun Lu, Brian C. Hosler, Lars Hultman, Paul R. C. Kent, Yury Gogotsi, and Michel W. Barsoum, *ACS Nano* 2015 *9* (10), 9507-9516. DOI: 10.1021/acsnano.5b03591. Copyright 2015 American Chemical Society.[21]

Chapter 2:

MoAlB Powder Synthesis

2.1 Introduction

MAB phases are traditionally synthesized in a variety of ways such as by aluminum flux, arc-melting, hot and cold-pressing the materials, and spark-plasma sintering.[21] All of these methods involve relatively complex equipment that is expensive, requires extensive knowledge and experience in solid-state chemistry, and many require post-synthetic steps to access the desired material. The aluminum flux method, one of the simplest synthetic methods, precipitates single crystals from a molten aluminum flux after heating in a furnace for an extensive period. When removed from the flux, the crystals are encased in an aluminum shell. This method also requires an aluminum digestion step that can be dangerous and time consuming. Residual aluminum flux media and aluminum-containing intermetallics are present as impurities that require the use of a high concentration of hydrochloric acid to remove. Despite treatment with hydrochloric acid, some impurities remain. Some MAB phases are very acid stable, including MoAlB, while others, such as Fe_2AlB_2, are not. Thus, in these cases, digestion of the flux media is not selective and results in a decreased yield. After all of the crystals are separated from the acid solution, the crystals need to be mechanically separated

from the leftover acid-stable byproducts by hand. This is a tedious step that slows down the production since the crystals cannot be separated through other properties, such as magnetism. Collectively, these factors make the flux growth of MAB phase single crystals less attractive than synthetic methods that do not rely on a large excess of aluminum. An alternative synthetic method is needed to facilitate the synthesis and subsequent experimental studies of MoAlB and related MAB phases. The following sections describe a method that I developed for the synthesis of MoAlB powder that is facile, scalable, and results in a relatively pure product.

2.2 Experimental

2.2.1 Materials:

To synthesize the powdered form of MoAlB, Fe_2AlB_2, WAlB, Ni_2AlB_2, and Co_2AlB_2 the following chemicals were purchased and used without further purification: MoB (Alfa Aesar, 99.5 %), FeB, (Alfa Aesar, 98%), WB (Sigma-Aldrich, 99%), NiB (Sigma-Aldrich, 99%, contains Ni_4B_3), Co_2B-Co_3B (Alfa Aesar, 99%), Al chips (NOAH Technologies, 99.99%), Titanium foil (Sigma-Aldrich, 99.7%, 0.25 mm, trace metals basis),and Zr foil (Sigma Aldrich, 99.2%, 1 mm). The crucible used was a 2 mL alumina crucible (Coorstek).

2.2.2 Procedure:

MoAlB Powder Synthesis. Powdered MoAlB was synthesized using a 1:1.3 ratio of MoB to aluminum chips (1505.4 mg MoB, 494.6 mg Al) in a 2-gram sample size, loaded into an alumina crucible, and placed in a Carbolite Tube Furnace Up to 1500 ^{o}C - STF/TZF within a mullite tube. A small piece of Zr foil was added upstream of the alumina crucible in the tube furnace to help avoid the formation of Al_2O_3 in the system. This mixture was heated under argon flow in a tube furnace for approximately 36 hours. The tube was flushed with argon for 10 min before the temperature was increased to 1400 °C at 2.5 °C / min. The heating profile for this sample continued as follows: dwelled at 1400 °C for 10 hours, cooled to 900 °C at 1 °C / min, cooled to 300 °C at 3 °C / min, and lastly cooled to room temperature at 1 °C / min. At this time the gas was automatically shut off. The sample was then mechanically separated from the crucible with a hammer and ground into a powder for use with an agate mortar and pestle. Pictorial representation of the procedure can be found in Figure 3.

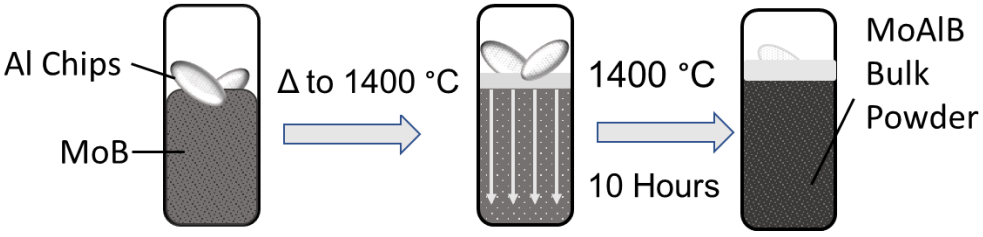

Figure 3: Schematic of MoB:Al chips 1:1.3 powder synthesis

[Recommendations for Syntheses: It is crucial that the binary boride powder is placed below the aluminum chips in this process, so the liquid aluminum can

proceed through the powder phase. Otherwise, the product will be a mixture of phases and not the desired lightly sintered material.]

MoAlB Single Crystal Synthesis. MoAlB single crystals were prepared using a modification of a reported procedure from Okada *et al*.[22] Mo powder (SigmaAldrich, 99.99%), B powder (Alfa Aesar, 98%), and Al chips (NOAH Technologies, 99.99%) were added to a 2 mL alumina crucible (Coorstek) in a Mo:Al:B 1:53.3:1 molar ratio. Each sample is prepared on a scale of 2 g total weight (124.2 mg Mo, 1861.8 mg Al, and 14.0 mg B). The crucible was then placed into a Carbolite Tube Furnace Up to 1500 ºC - STF/TZF with a mullite tube. The tube was flushed with argon for 10 min before the temperature was increased to 1400 °C at 2.5 °C / min. The heating profile for this sample continued as follows: dwelled at 1400 °C for 10 hours, cooled to 900 °C at 1 °C / min, cooled to 300 °C at 3 °C / min, and lastly cooled to room temperature at 1 °C / min. The excess flux medium was digested in 3 M HCl at room temperature to yield MoAlB single crystals. Pictorial representation of the procedure can be found in Figure 4.

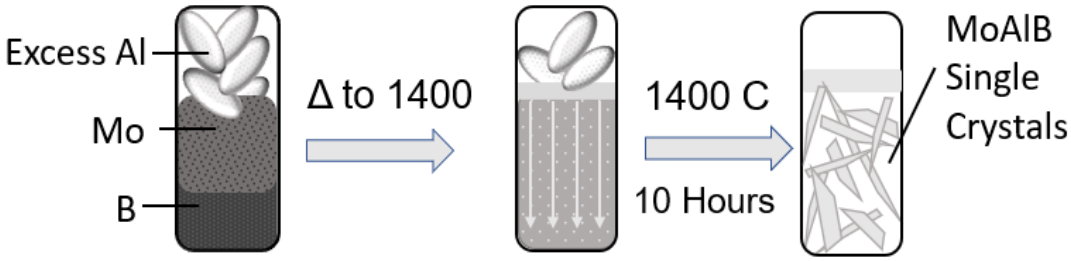

Figure 4: Schematic of Mo:Al chips:B 1:53.3:1 single crystal synthesis

Fe_2AlB_2 Powder Synthesis. Powdered Fe_2AlB_2 was synthesized using a 1:1.3 ratio of FeB to aluminum chips in a 2-gram sample size (1310.4 mg FeB,

689.6 mg Al chips), loaded into a 2 mL alumina crucible. A small piece of Zr foil was added near the alumina crucible in the Carbolite Tube Furnace Up to 1500 ºC - STF/TZF within a mullite tube to help avoid the formation of Al_2O_3 in the system. This mixture was heated under argon flow in a tube furnace for approximately 44 hours. The heating profile for this sample was as follows: from ambient temperature and pressure heated to 1400 °C at 2.5 °C / min, dwelled at 1400 °C for 18 hours, cooled to 900 °C at 1 °C / min, cooled to 300 °C at 3 °C / min, and lastly cooled to room temperature at 1 °C / min. At this time the gas was automatically shut off. The sample was then mechanically separated from the crucible and ground into a powder for use.

WAlB Powder Synthesis. Powdered WAlB was attempted to be synthesized using a 1:2.5 ratio of WB to aluminum chips in a 2-gram sample size (1485.3 mg WB, 514.7 mg Al chips), loaded into a 2 mL alumina crucible The alumina crucible was loaded into the Carbolite Tube Furnace Up to 1500 ºC - STF/TZF within a mullite tube. This mixture was heated under argon flow in a tube furnace for approximately 44 hours. The heating profile for this sample was as follows: from ambient temperature and pressure heated to 1400 °C at 2.5 °C / min, dwelled at 1400 °C for 18 hours, cooled to 900 °C at 1 °C / min, cooled to 300 °C at 3 °C / min, and lastly cooled to room temperature at 1 °C / min. At this time the gas was automatically shut off. The sample was then mechanically separated from the crucible and ground into a powder for use.

Ni_2AlB_2 Powder Synthesis. Powdered Ni_2AlB_2 was attempted to be synthesized using a 2:1.5 ratio of NiB to aluminum chips in a 2-gram sample size (1549.0 mg NiB, 451.0 mg Al chips), loaded into a 2 mL alumina crucible. The alumina crucible was loaded into the Carbolite Tube Furnace Up to 1500 ^{o}C - STF/TZF within a mullite tube. This mixture was heated under argon flow in a tube furnace for approximately 44 hours. The heating profile for this sample was as follows: from ambient temperature and pressure heated to 1400 °C at 2.5 °C / min, dwelled at 1400 °C for 18 hours, cooled to 900 °C at 1 °C / min, cooled to 300 °C at 3 °C / min, and lastly cooled to room temperature at 1 °C / min. At this time the gas was automatically shut off. The sample was then mechanically separated from the crucible and ground into a powder for use.

Co_2AlB_2 Powder Synthesis. Powdered Co_2AlB_2 was attempted to be synthesized using a 1:1.3 ratio of Co_2B-Co_3B (Co_3B was used for the ratio calculation) to aluminum chips in a 2-gram sample size (1645.1 mg Co_3B, 354.9 mg Al chips), loaded into a 2 mL alumina crucible. The alumina crucible was loaded into the Carbolite Tube Furnace Up to 1500 ^{o}C - STF/TZF within a mullite tube. This mixture was heated under argon flow in a tube furnace for approximately 44 hours. The heating profile for this sample was as follows: from ambient temperature and pressure heated to 1400 °C at 2.5 °C / min, dwelled at 1400 °C for 18 hours, cooled to 900 °C at 1 °C / min, cooled to 300 °C at 3 °C / min, and lastly cooled to room temperature at 1 °C / min. At this time the gas was automatically shut off. The sample was then mechanically separated from the crucible and ground into a powder for use.

Preparation of Powdered MoAlB Working Electrodes. The MoAlB that was synthesized as a powder was used in this preparation of the working electrodes for HER catalysis. A stock suspension of ~2 mg / mL of a MoAlB powder and ethanol was made and was slowly dropped onto a 0.25 cm^2 piece of titanium foil. After one drop was cast, the foil that was now coated with some MoAlB was dried under ambient conditions. Once dried, the MoAlB-coated titanium foil was annealed under forming gas (5% H_2 95% Ar) for 5 hours at 400 °C. Sn-plated Cu wires were fastened to the annealed titanium foil via Ag paint that could dry overnight. Once dried, all surfaces on the electrode that did not have MoAlB powder on them were covered with two-part epoxy. This includes the metal wire and uncovered edges of titanium foil as seen in Figure 5.

Figure 5: MoAlB Directly Synthesized Powder Working Electrode

Preparation of Single Crystal MoAlB Working Electrodes. The MoAlB that was synthesized as crystals was used in this preparation of the working electrodes for HER catalysis. The single crystals were ground using a mortar and pestle until a very fine powder was achieved. A stock suspension of ~2 mg / mL of a MoAlB powder and ethanol was made and was slowly dropped

onto a 0.25 cm^2 piece of titanium foil. After one drop was cast, the foil that was now coated with some MoAlB was dried under ambient conditions. Once dried, the MoAlB-coated titanium foil was annealed under forming gas (5% H_2, 95% Ar) for 5 hours at 400 °C. Sn-plated Cu wires were fastened to the annealed titanium foil via Ag paint that could dry overnight. Once dried, all surfaces on the electrode that did not have MoAlB powder on them were covered with two-part epoxy. This includes the metal wire and uncovered edges of titanium foil. Photographs of the electrode can be found in Figure 6.

Figure 6: MoAlB Ground Single Crystals Working Electrode

Electrochemical measurements. All electrochemical measurements were conducted on a Gamry Instruments Reference 600 potentiostat in a single compartment, four-necked round bottom flask using a 0.5 M H_2SO_4 solution. Three electrodes were used in each experiment where one of them was the working electrodes described above, the second was a graphite electrode, and the last one was a saturated calomel electrode (SCE).

2.2.3 Characterization:

Powder X-ray diffraction (XRD) patterns were acquired using a Bruker-AXS D8 Advance diffractometer with Cu Kα radiation and a LynxEye 1-D detector. SEM data was collected on a FEI NOVA Nano SEM 630 instrument with a 5 kV accelerating voltage and 3 mm working distance. The single crystal samples were placed on an SEM stub that was covered by carbon tape (TED PELLA) so they would lay flat. The MoAlB direct powder synthesis product was added to an analogous carbon tape covered SEM stub by lightly dusting the stub with powder. It was allowed to sit for a 1 minute then the excess powder was gently tapped off.

2.3 Results and Discussion

2.3.1 Synthetic Results for MoAlB and Fe_2AlB_2.

A reliable approach to synthesize phase pure MoAlB was successfully established, as seen in Figure 7. The ground sample was characterized using powder X-ray diffraction (XRD), scanning electron microscopy (SEM), and electron dispersive spectroscopy (EDS). The major phase observed in all characterization techniques was consistent with the expected ternary boride. However, there were small alumina and MoB impurities in the MoAlB samples that can be considered minor phases that have a minimal impact on the HER catalysis and the etching studies.

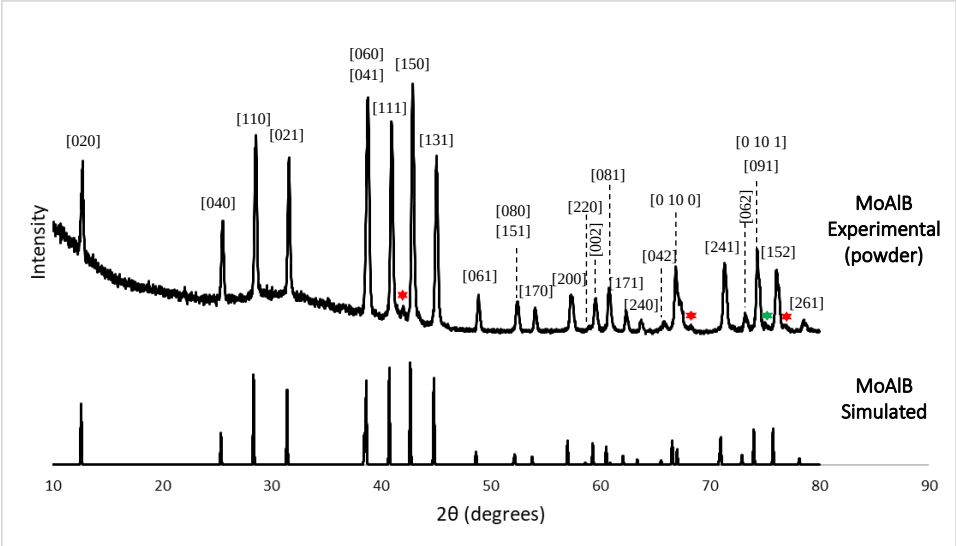

Figure 7: Experimental powder XRD pattern for MoAlB. Red stars (*) indicate rhombohedral corundum (Al_2O_3) and the green star (*) indicates tetragonal MoB; all other peaks are MoAlB.

SEM with EDS analysis confirmed that the ratios between all three elements in each phase match the ratios expected for the desired ternary boride phase. Rietveld refinement was performed for this direct powder synthesis of MoAlB using the GSAS II software suite.[23] The phases that were confirmed using the refinement were MoAlB, Al_3Mo, and Al_2O_3. The Al_2O_3 phase was confirmed from the quantitative analysis of the XRD pattern shown in Figure 8. The relative percent of each phase in the system was 88% MoAlB, 3% Al_3Mo, and 9% Al_2O_3. These relative percentages are comparable to other percentages found in literature that are on average in the mid-high nineties for the MoAlB phase as well as same 3% for Al_3Mo.[24] They are not as high as the literature values that stem from less accessible synthetic procedures (i.e. procedures that require a hot press), but they are superior to other highly accessible techniques for powder synthesis.

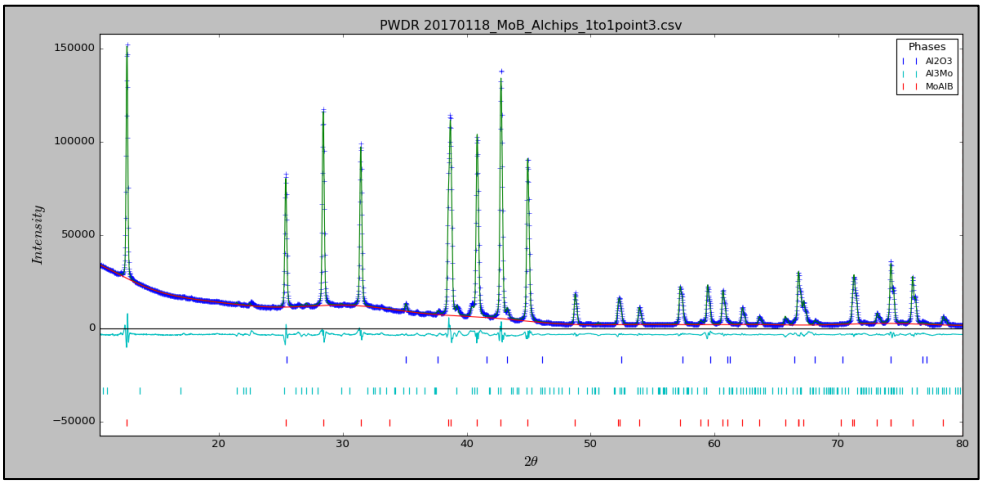

Figure 8: Rietveld refinement of direct powder synthesis for MoAlB (red) with peak positions for Al_2O_3 (blue) and Al_3Mo (green) also indicated.

When comparing Figure 7 and Figure 8 there is a difference in the impurities seen between them. This is because the Rietveld refinement was done on an earlier sample in the lifetime of this project. The main difference between the two samples is the addition of the Zr getter which was present in Figure 7 but not Figure 8. The impurities may have changed slightly between the addition of this getter, but the main source of error for the sample to sample variation comes from the weight measurement of the aluminum chips. The Figure 7 sample likely had a slightly lower ratio of Al chips to MoB leading to the formation of MoB or leaving some unreacted. However, Figure 8 likely had a slightly higher amount of Al chips added causing an aluminum intermetallic to form from the excess aluminum. This was added to the report to emphasize the importance of precise measurement and sample to sample variability.

Fe_2AlB_2 was able to be synthesized as well, but there were many binary intermetallics that were found to accompany the ternary boride in all syntheses. The purity of Fe_2AlB_2 can be seen in Figure 9 by comparing the reference pattern to the experimental pattern below.

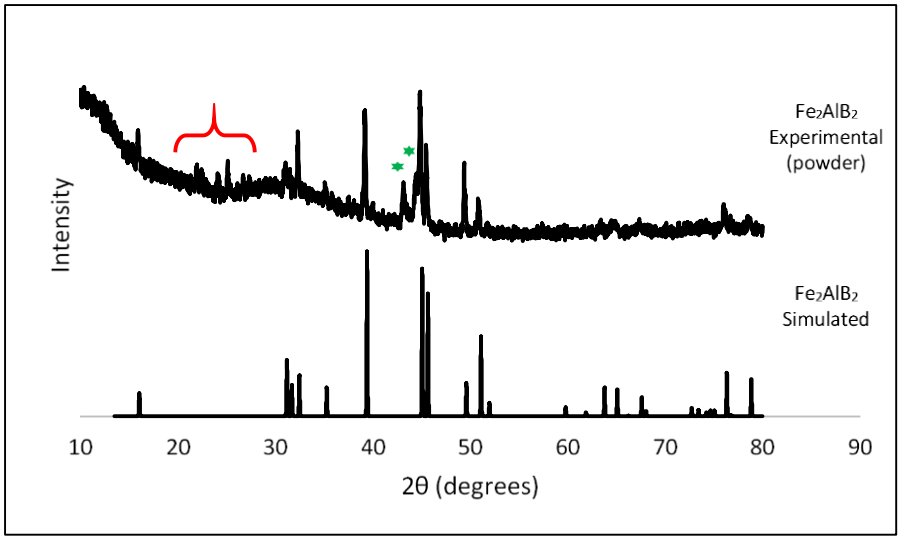

Figure 9: Simulated Fe_2AlB_2 XRD pattern compared to the experimental powder form of the sample. Impurities are marked with asterisks. Peaks under the red bracket indicate monoclinic $Al_{13}Fe_4$ and green asterisks (*) indicate tetragonal Fe_3B. All other peaks correspond to orthorhombic Fe_2AlB_2.

A key experimental change in this report that is different from Okada's original approach to synthesize MoAlB and Fe_2AlB_2 single crystals is the use of Zr foil to mitigate oxide formation. In these studies, it was imperative to use the Zr foil, also known as an oxygen getter, due to the formation of aluminum oxide (alumina) that formed along with the MoAlB powder. Figure 10 below shows the presence of a peak diagnostic of alumina near 35º 2-theta. This figure also shows a side-by-side comparison of MoAlB synthesized using no Zr getter (left) and with a Zr getter (right). Incorporating Zr foil upstream of the alumina crucible helps to prevent the formation of alumina, because the Zr reacts with residual oxygen to remove it from the tube, thereby decreasing the amount of oxygen available to react with aluminum.

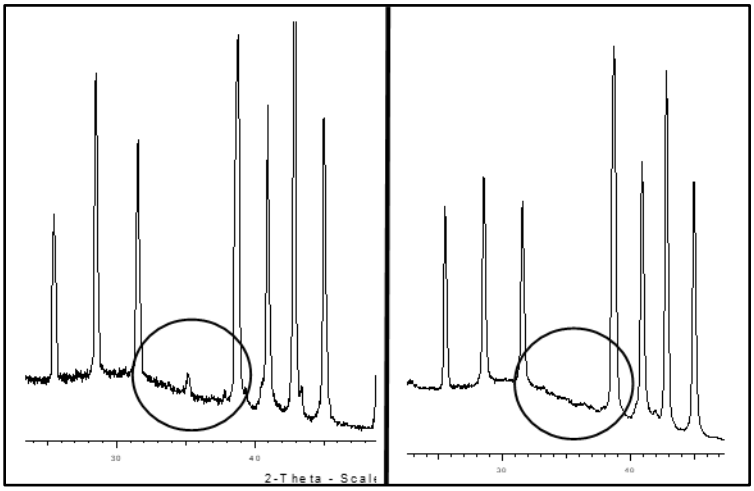

Figure 10: Experimental MoAlB XRD pattern with no Zr getter (left) and with Zr getter (right) where the most prominent alumina peak is circled.

The size of the Zr foil was also varied, and it was found that a roughly 1 cm^2 x 1 cm^2 piece was the optimal amount. Zr foil areas larger than 1 cm^2 did not decrease the amount of the oxides that formed.

Throughout this project multiple different M metals in the MAB phases were tested to be adapted to this procedure. MoAlB and Fe_2AlB_2 were found to be successful in producing analogous phases to the single crystal syntheses. However, metals other than Mo and Fe were studied as well, including Ni, W, and Co. The XRD for each respective newly tried metal is seen in Figure 11.

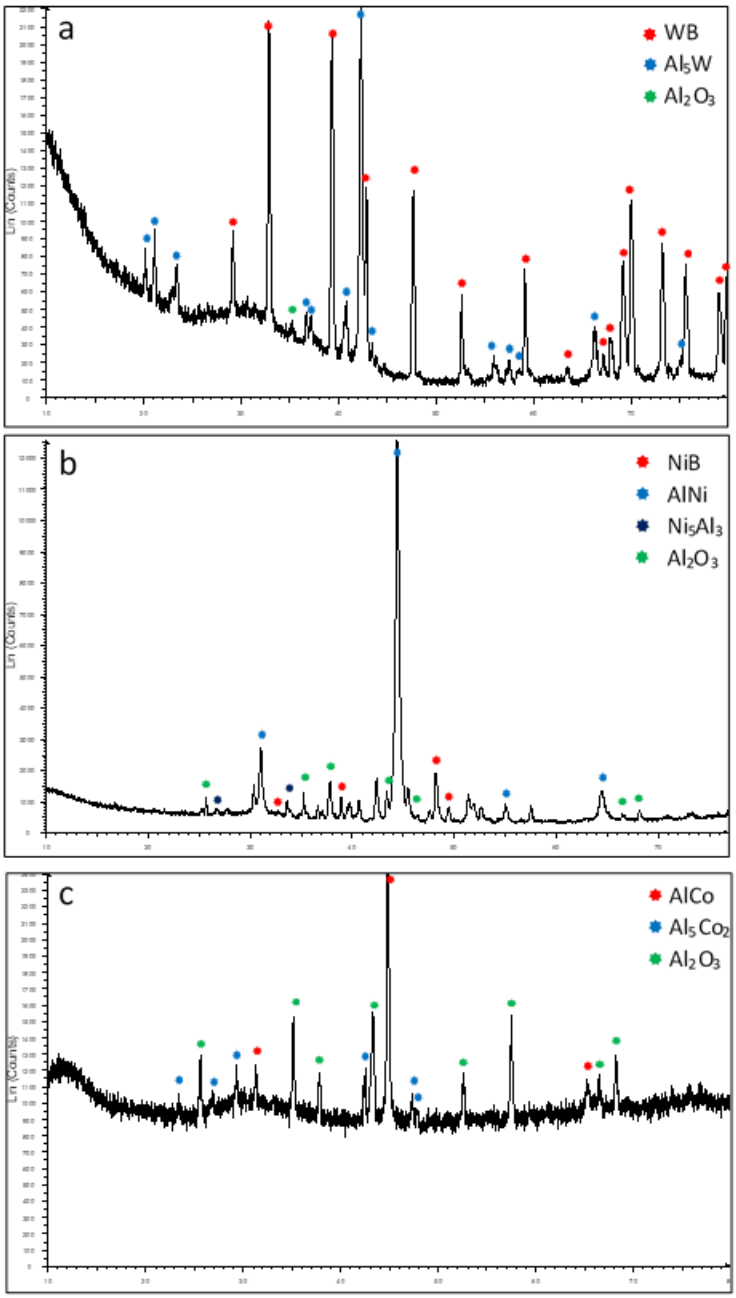

Figure 11: Experimental XRDs showing the attempts at synthesizing WAlB (a), Ni_2AlB_2 (b), and Co_2AlB_2(c) via the direct powder synthesis. Panel (a) shows tetragonal WB, hexagonal Al_5W, and rhombohedral Al_2O_3. Panel (b) shows orthorhombic NiB, cubic AlNi, orthorhombic Ni_5Al_3, and rhombohedral Al_2O_3. Panel (c) shows hexagonal Al_5Co_2, cubic AlCo, and rhombohedral Al_2O_3.

Each of these syntheses did not produce any of the desired ternary boride phase. All of the phases found were aluminum intermetallics, aluminum oxides or the binary boride used in the synthetic approach with the exception of the cobalt sample, i.e. WB, and NiB. Each M element tried would be great avenues to pursue in the future as these contain elements of interest for the field due to the potential for properties not commonly exhibited by the related class of MAX phases, such as magnetic properties.

2.3.2 HER in Acid Conditions.

The directly synthesized MoAlB powder was tested for its ability to catalyze hydrogen evolution in comparison to the single crystal synthesis product. The single crystal product was already synthesized, made into electrodes, and published in the earlier reporting by Alameda *et al*.[25] Fe_2AlB_2 was not tested due to the presence of multiple byproducts in the final syntheses. As mentioned in the procedure section above, the single crystal MoAlB was ground into a fine powder to mimic the state of the directly synthesized MoAlB powder. This was done because Alameda *et al.* found that the basal planes of the MoAlB single crystals were more active than the edge sites.[25] Figure 12 shows an image of a MoAlB single crystal and powder.

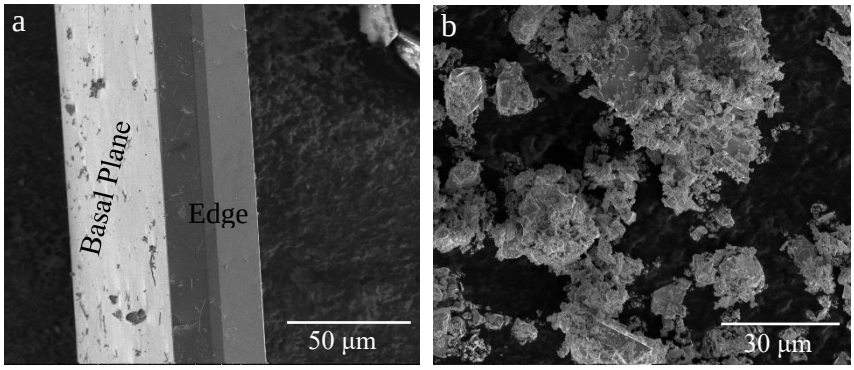

Figure 12: MoAlB single crystal (a) and directly synthesized powder (b). These crystals have a coffin-like shape with the flat basal plane taking up the majority of the area and the much smaller surface area edges. However, the powder has no distinct crystal morphology from SEM. Grinding up the powder would ensure that the same overall surface area was achieved as well between the samples.

It was found that the direct powder synthesis of MoAlB produced a catalyst having slightly better performance than the MoAlB synthesized as the ground single crystals. Three electrodes were tested for each sample type. MoAlB synthesized directly as a powder showed HER activity with an overpotential near 470 mV at 1 mA / cm^2 and the ground single crystal MoAlB showed an overpotential of 457 mV at 1 mA / cm^2, as seen in Figure 13. The overpotentials are not reported at the standard 10 mA / cm^2 current density because the electrode did not reach that current density before surpassing useful overpotentials.

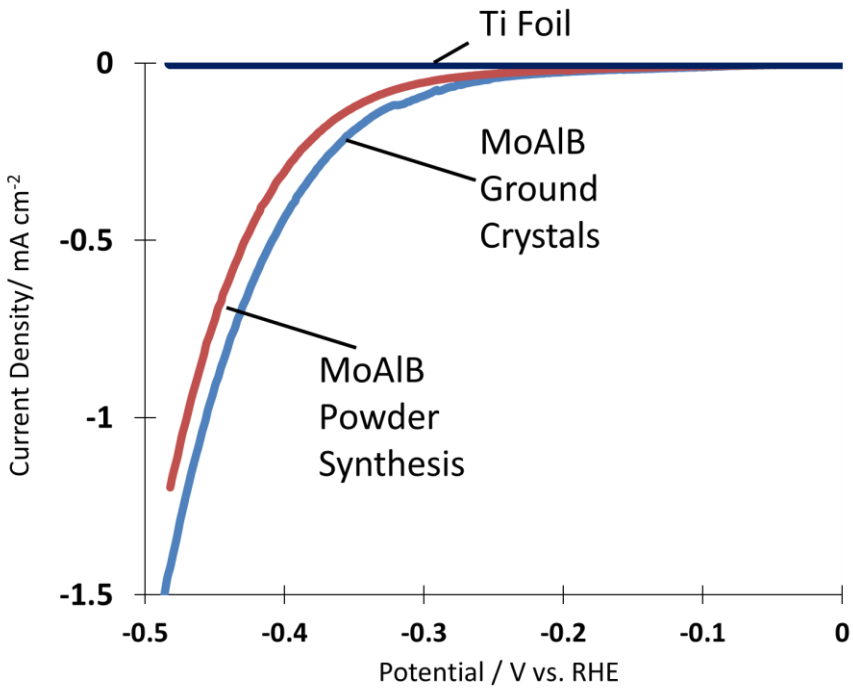

Figure 13: Polarization data for HER catalysis in 0.5 M H_2SO_4 for MoAlB direct powder synthesis (red) and MoAlB ground single crystals (blue) with a Ti wire for comparison (black).

The previous report of MoAlB, that this section of work was inspired by, was an experiment to investigate the catalytic activity of MoAlB's basal planes and the combination of basal planes and edges together to learn if there was a difference between their activities. An additional motivational point behind this paper was to compare the HER activities of MoAlB structural variations with etched material. The etching of MoAlB will be discussed more in Chapter 3. The data that Alameda *et al.*[25] first reported showed that edge sites have a lower catalytic activity compared to basal planes in MoAlB. This was tested by creating single crystal electrodes, described above, having only the basal plane exposed and with both edge sites and basal planes exposed to the acidic medium. The

same electrochemical testing procedure was conducted between each electrode and it was repeated several times.

The overpotential reported by Alameda *et al.*[25], with the basal plane only exposed, ranged between 360-390 mV at 10 mA / cm^2. The combination of edge sites and basal plane were measured to have an overpotential near 400 mV at 10 mA / cm^2. With this data, the conclusion was made that edge sites reduce the HER activity of MoAlB single crystals. This same conclusion is proposed to be the reasoning for why the experimental data collected for the direct powder synthesis and ground single crystal data are so low. When the single crystals are ground up, the ratio of basal planes to edges is decreased significantly due to the particles becoming more isotropic (less plate-like) upon grinding. This decreases the catalytic activity of the overall substance and explains the overall trend seen for the decrease of the ground crystals to the original report. The direct powder synthesis shows a similar result, but this sample performs better than the ground single crystals

2.4 Conclusion

In conclusion, an easier synthetic approach to synthesize one ternary boride phase has been successful as well as the testing of that ternary boride for HER. This new method will allow for the expansion of this field due to its simplicity, scalability, and independence from complex solid-state chemistry equipment. The use of commercially available precursors allows for easy

preparation for the synthesis as well as it significantly cuts down the amount of total time needed to prepare a powder sample. MoAlB can be produced in very similar purity to the previously preferred aluminum flux crystal synthesis, as well as the other synthetic methods of hot and cold-pressing, arc-melting, and spark plasma sintering with the addition of the zirconium foil. The next steps will be to synthesize other ternary borides with this method to further advance the various synthetic pathways to achieving a MAB phase. This work was later used as the synthesis portion of a paper co-authored by Alameda and myself.[26]

It was found that the HER activity of the MoAlB produced by this new synthetic method is much less active than its non-powder single crystal counterpart. However, when the single crystals are ground and tested in the same powder form as the new synthetic material, it results in an overall lower activity for HER than the direct powder synthesis. This is consistent with previous report by Alameda *et al*. and underlines the importance of the relationship between morphology and active sites (i.e. which facets are the active sites located on and to what degree does the morphology of the material expose those facets) to catalytic design. It is certain that this new synthetic prep will give access to MoAlB easier than ever, but it does not appear to facilitate HER activity in the material.

Chapter 3:

Exploration of New Etching Pathways for MoAlB

3.1 Introduction

Etching has been the primary chemical method to transform 3D MAX phases into 2D MXenes,[27] and it is also the approach being explored to access the theoretical MBene from MAB phase precursors. The main hurdle that has been encountered comes from the incomplete etching of MoAlB. The paper by Alameda *et al.*[25] describes this partial etching where there are visible etched cavities in the single crystals, but the EDS analysis shows a very small difference in the Mo:Al:B ratio, which suggests that only partial etching of the crystals occured.[11, 25] This prompted the exploration into different procedures to etch MAB phases to discover a condition to make MBenes that is distinct from MXenes, because the conditions used to synthesize MXenes do not appear to produce MBenes from MAB phases. Literature that references ways to etch MAX phases mention the use of hydrogen fluoride (HF) based etching solutions either with the use of HF directly or *in situ* HF via most commonly LiF and HCl.[23] This procedure is both dangerous and very corrosive to MoAlB due to the fluoride ions used to etch the material which makes it unsuitable for MAB phases.[26] A new procedure that utilizes an etchant that is safer for the user and non-corrosive to the MAB phase would be an ideal candidate. The combination

of the desire to form 2D MoB and the previously mentioned new synthetic pathway to make MoAlB directly into a powder, sparked interest in a new approach to etch MAB phases.

3.2 Experimental

3.2.1 Materials

To synthesize the powdered form of MoAlB the following chemicals were purchased and used without further purification: MoB (Alfa Aesar, 99.5 %), Al chips (NOAH Technologies, 99.99%), and Zr foil (Sigma Aldrich, 99.2%, 1 mm). The crucible used was a 2 mL alumina crucible (Coorstek).

3.2.2 MoAlB Powder Synthesis

MoAlB Powder Synthesis. Powdered MoAlB was synthesized using a 1:1.3 ratio of MoB to aluminum chips (1505.4 mg MoB, 494.6 mg Al) in a 2-gram sample size, loaded into an alumina crucible, and placed in a Carbolite Tube Furnace Up to 1500 ^{o}C - STF/TZF within a mullite tube. A small piece of Zr foil was added upstream of the alumina crucible in the tube furnace to help avoid the formation of Al_2O_3 in the system. This mixture was heated under argon flow in a tube furnace for approximately 36 hours. The tube was flushed with argon for 10 min before the temperature was increased to 1400 °C at 2.5 °C / min. The heating

profile for this sample continued as follows: dwelled at 1400 °C for 10 hours, cooled to 900 °C at 1 °C / min, cooled to 300 °C at 3 °C / min, and lastly cooled to room temperature at 1 °C / min. At this time the gas was automatically shut off. The sample was then mechanically separated from the crucible and ground into a powder for use with an agate mortar and pestle. Pictorial representation of the procedure can be found in Figure 14.

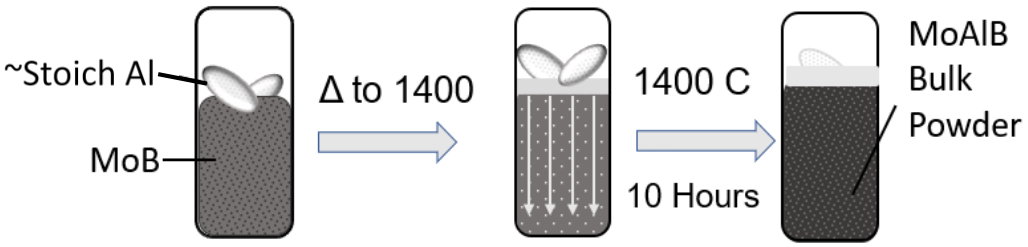

Figure 14: Schematic of MoB:Al chips 1:1.3 powder synthesis

[*Recommendations for Syntheses: It is crucial that the binary boride powder is placed below the aluminum chips in this process, so the liquid aluminum can proceed through the powder phase. Otherwise, the product will be a mixture of phases and not the desired lightly sintered material.]*

3.2.3 Etching

MoAlB from the direct powder synthesis was mechanically separated from the crucible with a hammer, and ground with an agate mortar and pestle. A sample of 200 mg of the ground MoAlB was submerged in 5 mL of 20% KOH at ambient conditions for 48 h with stirring.

3.2.3 Washing and Selective Precipitation

The powdered MoAlB was centrifuged (13,500 rpm, 2 min) to obtain a settled pellet of MoAlB powder. The excess liquid was decanted and replaced with DI water and sonicated to redispose and wash the settled powder. The etched MoAlB sample was then allowed to dry under a light air flow. *(Completion of 1 etch with no selective precipitation)*. Etched samples were suspended in 10 mL of DI water, sonicated until the solution was dispersed, then allowed to settle for 2-3 minutes (referred to as selective precipitation). The suspended particles were decanted and separated via centrifugation from solution. The suspended particles were dried under an air flow and reground. These etched particles were submerged in a 5 mL 20% solution of KOH for additional 48 h period iteratively until the desired number of etches were achieved. The larger particles were not used. Figure 15 describes the etching and washing cycle for how to iteratively etch and selectively precipitate the MoAlB.

Figure 15: Iterative etching and selective precipitation procedure.

Changing Etchant Cation

MoAlB as-synthesized powder was mechanically separated from the crucible with a hammer, ground with an agate mortar and pestle. A sample of 200 mg of the ground MoAlB was submerged in 5 mL of 20% NaOH or LiOH at ambient conditions for 48 h with stirring. Please refer to the 3.2.3 Washing and Selective Precipitation section for washing and selective precipitation procedure.

Decreased Concentration:

MoAlB as-synthesized powder was mechanically separated from the crucible with a hammer, ground with an agate mortar and pestle. A sample of 200 mg of the ground MoAlB was submerged in 5 mL of 10% KOH at ambient conditions for 48 h with stirring. Please refer to the 3.2.3 Washing and Selective Precipitation section for washing and selective precipitation procedure.

Increased Temperature:

MoAlB as-synthesized powder was mechanically separated from the crucible with a hammer, ground with an agate mortar and pestle. A sample of 200 mg of the ground MoAlB was submerged in 5 mL of 20% KOH at 45 ^{o}C for 48 h with stirring. Please refer to the 3.2.3 Washing and Selective Precipitation section for washing and selective precipitation procedure.

3.2.4 Characterization:

Powder X-ray diffraction (XRD) patterns were acquired using a Bruker-AXS D8 Advance diffractometer with Cu Kα radiation and a LynxEye 1-D detector. The CrystalMaker/CrystalDiffract software package was used to simulate XRD patterns for all binary borides as well as potential ternary borides.

3.3 Results and Discussion

3.3.1 Iterative Etching of MoAlB Powder.

A reproducible, iterative etching procedure has been developed to better understand the etching pathway of MoAlB. The iterative nature of the procedure is evident in the powder XRD data shown in Figure 16.

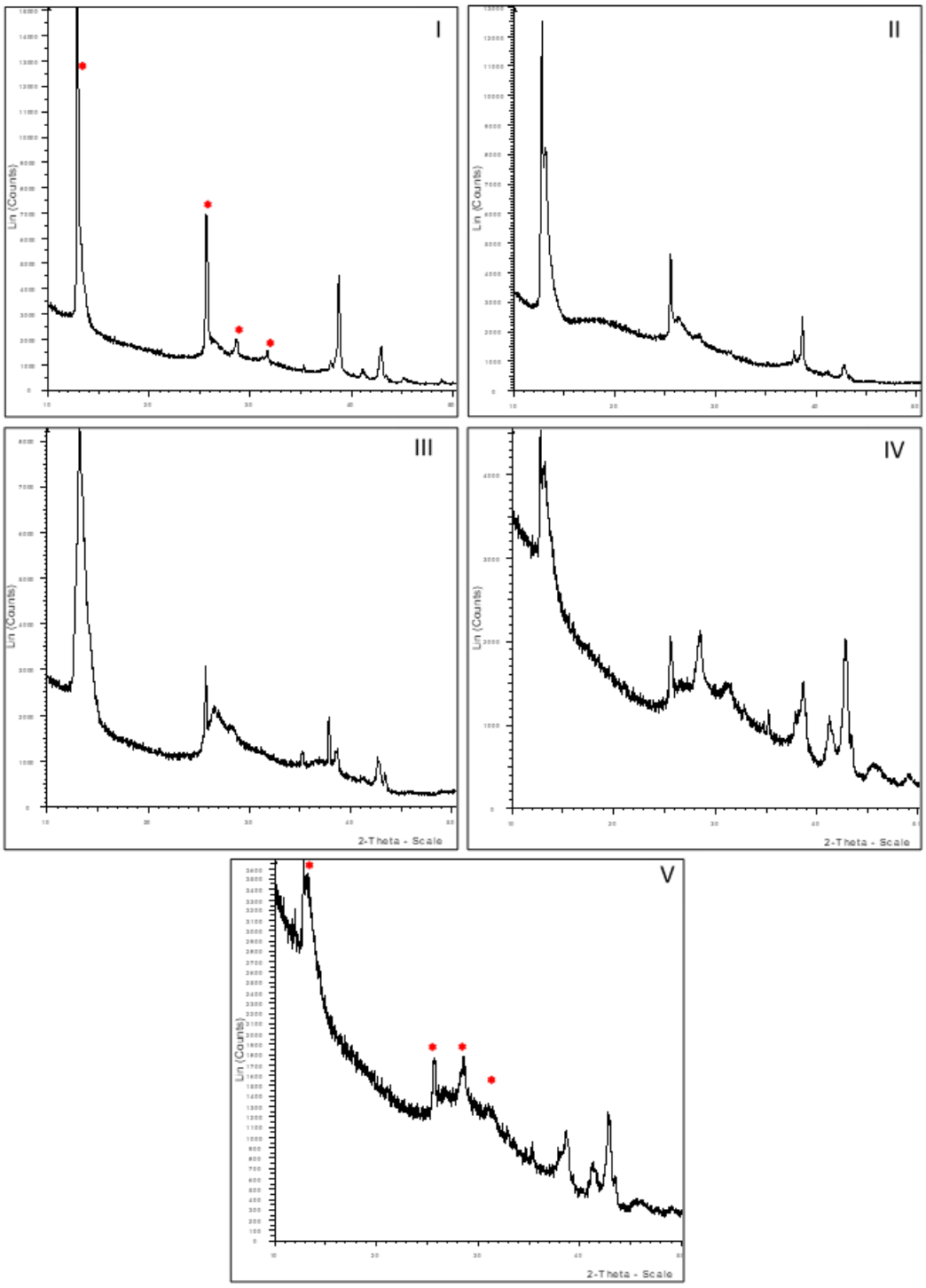

Figure 16: Powder XRD data for the iterative etching of MoAlB with 20% KOH for 48 hours where (I) is after the first etch and (V) is after the fifth etch. The large change in relative intensities can be seen by the red asterisks (*) at 13, 26, 28, & 31 2-theta

These successive etches of MoAlB with 20% KOH show a decrease in the crystallinity of the particles, demonstrated by the change in the relative intensities of four peaks at 13, 26, 28, and 31, 2-θ. These peaks likely signify a change in the MoAlB structure that will be discussed in greater detail in the 3.3.3 Role in Subsequent Research section of this thesis. The specific change in intensity of the [0k0] peaks is because of preferred orientation where it is more stable for them to lay on their basal planes than edges when the powder is analyzed with XRD.

3.3.2 Testing Etchant Type, Concentration, and Temperature Affects.

The previous work done by this group concentrates itself on 10% NaOH as the primary etchant type and concentration.[25, 26] This section of this thesis experiments with different etchant types and concentrations to determine if the 20% KOH solution has any impact on the results seen in the XRD.

The procedure for a singular etch was carried out with two additional etchants to determine how the results depend on the cation present. The 20% KOH was directly replaced with 20% NaOH and 20% LiOH solutions as the etchants shown in Figure 17.

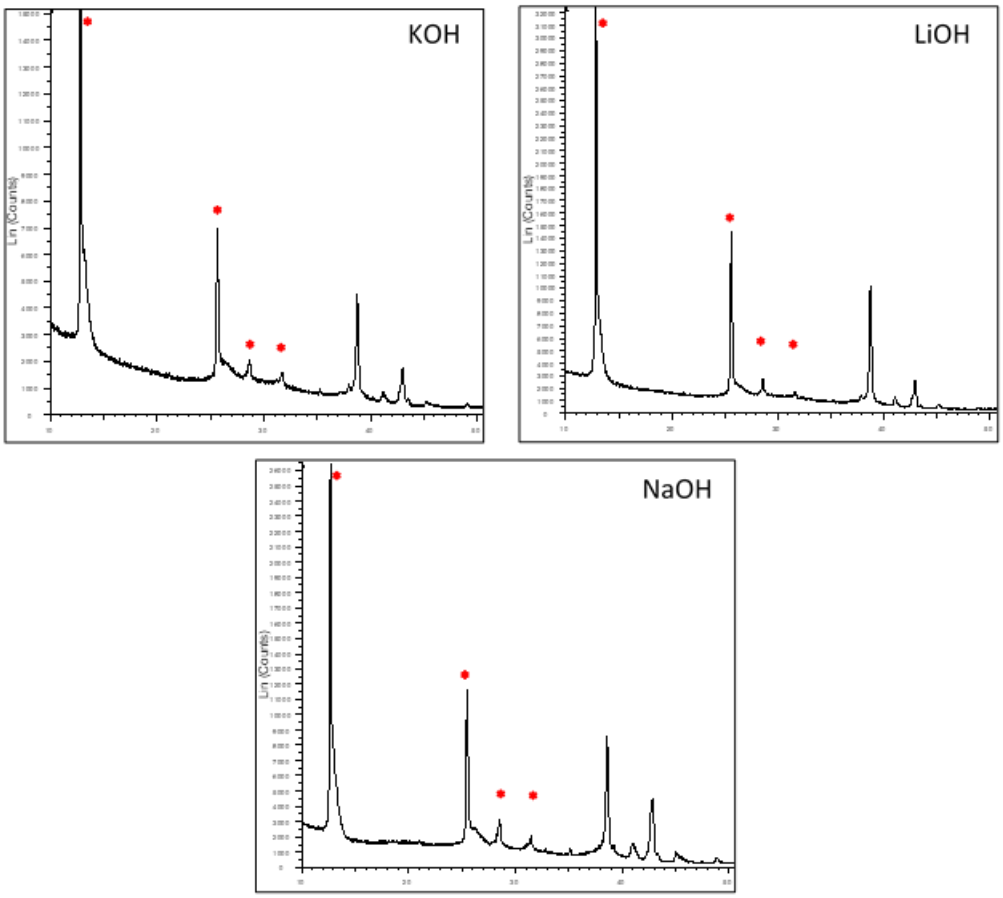

Figure 17: Powder XRD data for the iterative etching of MoAlB with 20% NaOH and 20% LiOH for 48 hours where first etch is pictured. The similar large change in relative intensities can be seen by the red asterisks (*) at 13º, 26º, 28º, & 31º 2-theta.

The substitution of NaOH or LiOH instead of KOH did not alter the relative intensities or positions of the XRD peaks. The change in the XRD patterns suggest that the sample is losing its crystallinity due to the broadening of the peaks, and a chemical change occurring mainly to the [0k0] peaks due to etching. Although it is not as apparent in the sample that was only etched once, it can be seen mainly in the 13 and 26 2-theta peaks. Each of the starred peaks in Figure 17 show the same relative amount of change respective to each base.

Additional tests were conducted to determine if concentration and temperature were factors in the degree of etching and structural changes previously observed. When comparing 10% and 20% KOH, no significant difference were observed in the XRD patterns (Fig. 18 and Fig. 19), which indicates that etchant concentration does not play and important role.

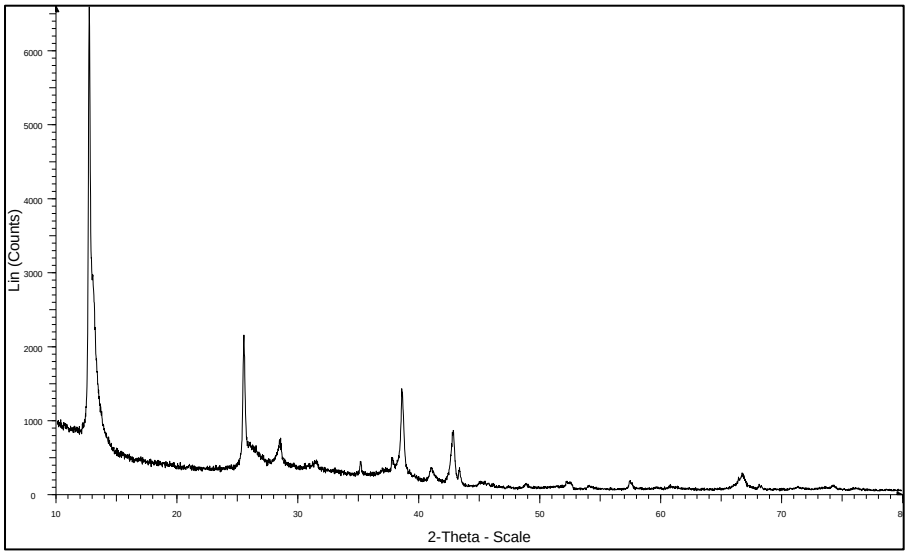

Figure 18: As synthesized MoAlB powder etched with 10% KOH for 48 hours.

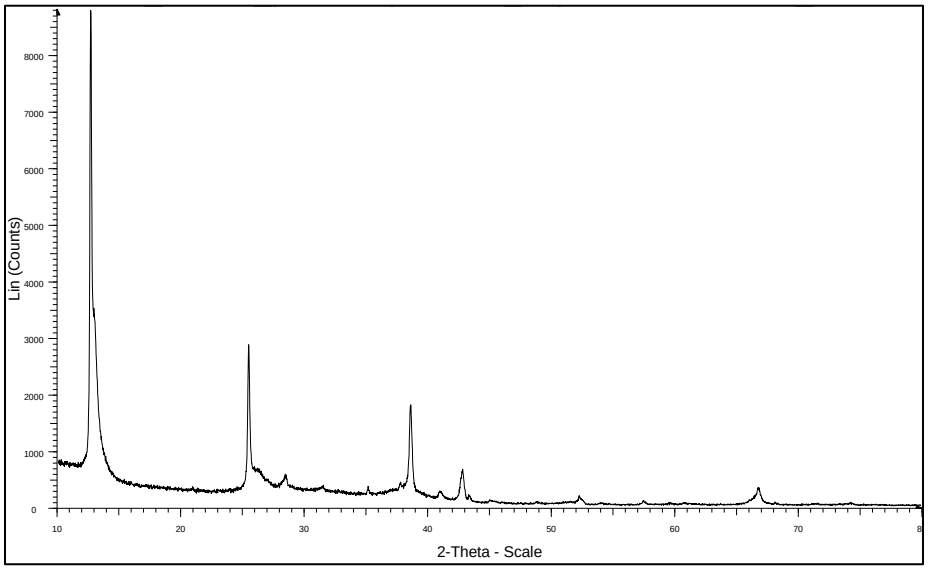

Figure 19: As synthesized MoAlB powder etched with 20% KOH for 48 hours.

The identical result was found for samples with increased temperature during etching as seen in Figure 20 where neither the intensities nor positions significantly changed in the XRD.

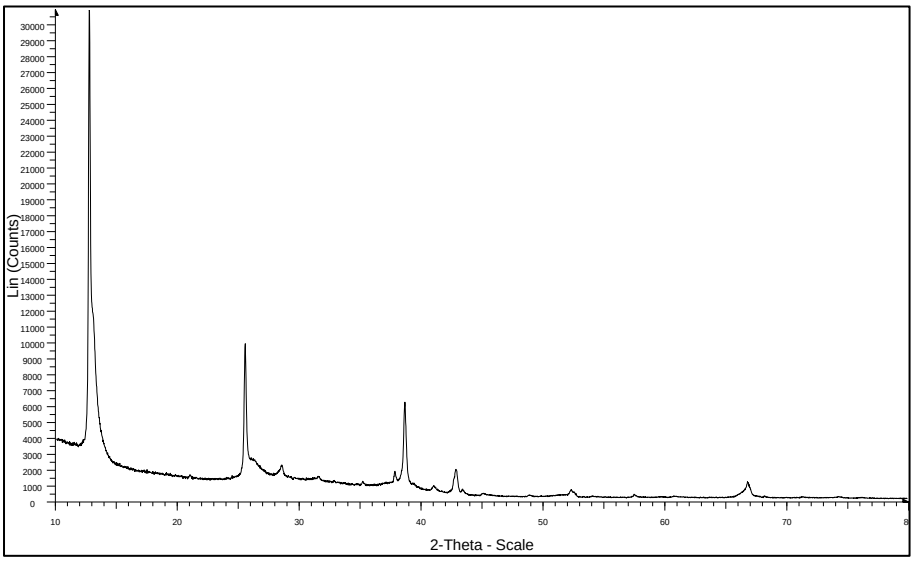

Figure 20: As synthesized MoAlB powder etched with 20% KOH at 45ºC for 48 hours.

Eliminating the etchant type, etchant concentration, and temperature effects as potential causes for the change found in the XRD patterns indicates that the etching behavior is not dependent on the etchant, but instead is dictated by a characteristic intrinsic to MoAlB.

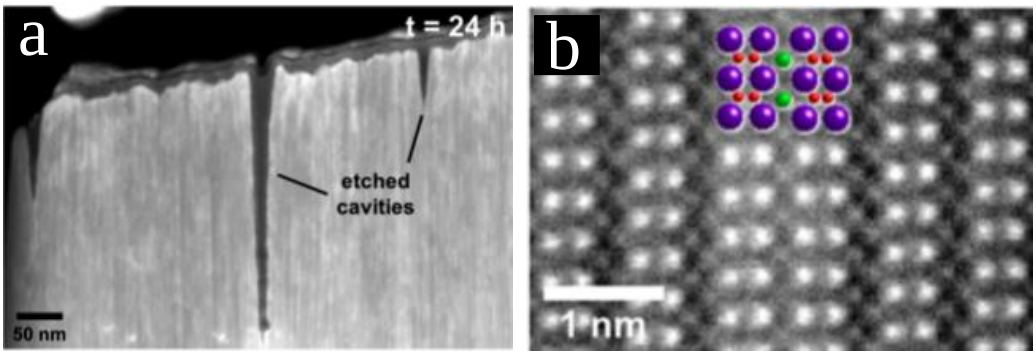

Figure 21: MoAlB single crystal etched by 10% NaOH for 24 hours showing etching cavities not fully penetrating the crystal. Adapted from Figure 2c and 4a of Alameda et al. "Topochemical Deintercalation of Al from MoAlB" paper.

Figure 21 shows a very small section of a much larger crystal in panel a with a few larger cavities and many white streaks showing stacking faults in the system. Panel b in Figure 21 shows an atomic resolution view of a MoAlB stacking fault (whiter sections in panel a) in the vertical orientation. The section of panel b directly to the left or right of the colored region shows normal stacking of MoAlB with two aluminum atoms staggered between each row of MoB units instead of the single line of aluminum atoms seen in green as seen in M_2AlB_2 type MAB phases. The iteratively etched particles that slowly decreased in particle size with each consecutive etch, allowed for a higher density of these etching cavities and stacking faults to occur because there is less bulk MoAlB to conflict with the signal. This made the XRD patterns exhibit the shift in intensity for the

specific peaks highlighted in Figure 16 since the etching mainly affects the (0k0) planes.[25]

3.3.3 Role in Subsequent Research

A recently published paper by myself and Alameda *et al*. details a method to access a hard-to-reach solid-state target, Mo_2AlB_2 by "translating low-temperature topochemical reactivity at surfaces and submicron regions to bulk systems."[28] This was a direct application of the previous section where selective precipitation and iterative etching were able to identify smaller particles with a higher density of stacking faults. This paper found that a metastable phase Mo_2AlB_2 can be derived from MoAlB when the smaller particles are etched, selectively precipitated, and then annealed at 600 ^{o}C for 4.5 hours with the overall scheme seen in Figure 22.

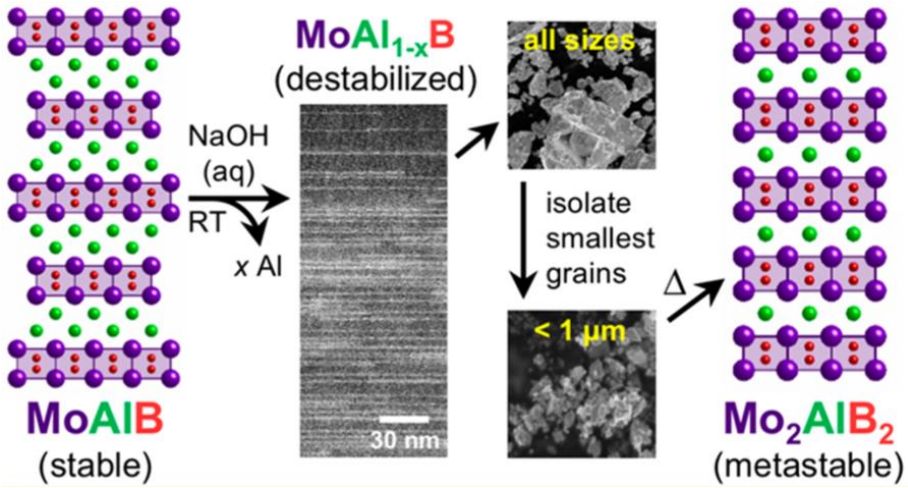

Figure 22: Overall topotactic scheme to synthesize Mo_2AlB_2 (adapted from paper by Alameda et al).[28]

The XRD pattern for Mo_2AlB_2 was simulated by Alameda et al. and is pictured below in Figure 23.

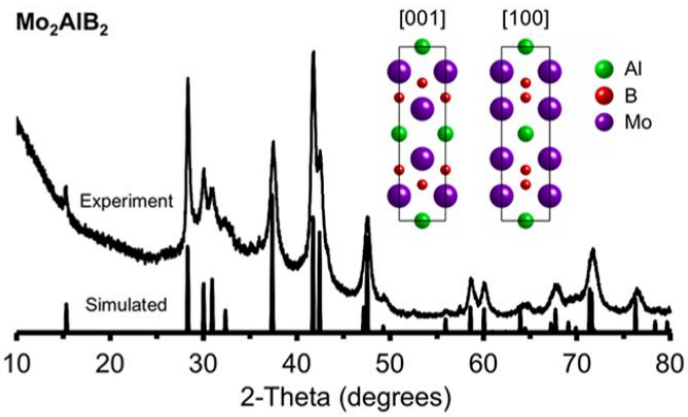

Figure 23: Powder XRD data of Mo_2AlB_2-AlO_x and simulated Mo_2AlB_2 (adapted from Alameda et al).[28]

This figure shows the next step in the process after the iterative etching process that was discovered. The iterative etching procedure requires a very large amount of as synthesized powder MoAlB that was discussed in Chapter 2 to be used in practice since only the smallest particles can be utilized. However, as a result of this work, it is now possible to produce an experimentally viable quantity of MoAlB powder.

3.4 Conclusion

In conclusion, a reproducible, iterative etching procedure has been developed to produce gram-scale MoAlB powder. This method has been tested through isolating three independent variables which has identified that the initial results are not dependent on the concentration of etchant, type of etchant, or the

time that the particle is exposed to the etchant. The results of these experiments showed changes in the relative intensities of the few highlighted peaks that can be attributed to a higher density of stacking faults in the (0k0) lattice planes. This discovery has allowed for the expansion of the field's understanding of MoAlB by leading to a paper by myself and Alameda *et al*.[28] detailing a MoAlB sub-type that forms when etched and annealed post-etching. The next steps to further progress this field will be to continue the development of post-synthetic and post-etching methods to achieve the elusive 2D MoB on a bulk scale.

BIBLIOGRAPHY

[1] Naguib, M.; Kurtoglu, M.; Presser, V.; Lu, J.; Niu, J.; Heon, M.; Hultman, L.; Gogotsi, Y.; Barsoum, M. W. Two-Dimensional Nanocrystals Produced by Exfoliation of Ti_3AlC_2. *Adv. Mater.* **2011**, *23*, 4248−4253.

[2] Xiaoyan Tan, Ping Chai, Corey M. Thompson, and Michael Shatruk
Journal of the American Chemical Society **2013** *135* (25), 9553-9557
DOI: 10.1021/ja404107p

[3] Vrubel, H.; Hu, X. Molybdenum Boride and Carbide Catalyze Hydrogen Evolution in both Acidic and Basic Solutions. *Angew. Chem*. 2012, 124, 12875−12878.

[4] Park, H.; Encinas, A.; Scheifers, J. P.; Zhang, Y.; Fokwa, B. P. T. Boron-Dependency of Molybdenum Boride Electrocatalysts for the Hydrogen Evolution Reaction. *Angew. Chem.* 2017, 129, 5667−5670.

[5] "Outlook for Energy: A Perspective to 2040." *ExxonMobil*, 28 Aug. 2019, corporate.exxonmobil.com/en/Energy-and-environment/Energy-resources/Outlook-for-Energy/2018-Outlook-for-Energy-A-View-to-2040#eyakeawaystlance.

[6] Cleveland, Cutler, and Christopher Morris. "Carbon-Based Fuel." *Carbon-Based Fuel - an Overview | ScienceDirect Topics*, 2014, ww.sciencedirect.com/topics/engineering/carbon-based-fuel.

[7] McAtee, C., McCullough, G., & Douglas, R. (2012). Performance and characteristics of platinum, palladium/rhodium and palladium automotive catalysts when subjected to ethanol, acetaldehyde and a synthetic E85 exhaust gas mixture. Proceedings of the Institution of Mechanical Engineers, Part D: *Journal of Automobile Engineering*, 226(11), 1536–1546. https://doi.org/10.1177/0954407012446911

[8] Eric J. Popczun, James R. McKone, Carlos G. Read, Adam J. Biacchi, Alex M. Wiltrout, Nathan S. Lewis, and Raymond E. Schaak
Journal of the American Chemical Society **2013** *135* (25), 9267-9270
DOI: 10.1021/ja403440e

[9] Mahmood, N., Yao, Y., Zhang, J.-W., Pan, L., Zhang, X., Zou, J.-J., *Adv. Sci.* 2018, 5, 1700464. https://doi.org/10.1002/advs.447

[10] Jahan, M., Liu, Z., Loh, K.P. (2013-11-20). A graphene oxide and copper-centered metal organic framework composite as a tri-functional catalyst for HER, OER, and ORR. *Advanced Functional Materials* 23 (43) : 5363-5372. ScholarBank@NUS Repository. https://doi.org/10.1002/adfm.201300510

[11] Novoselov, K. S., et al. "Electric Field Effect in Atomically Thin Carbon Films." *Science*, American Association for the Advancement of Science, 22 Oct. 2004, science.sciencemag.org/content/306/5696/666.

[12] Xin Zhao, Qinghua Zhang, Dajun Chen, and Ping Lu
Macromolecules **2010** *43* (5), 2357-2363
DOI: 10.1021/ma902862u

[13] R. Mas-Balleste , C. Gomez-Navarro , J. Gomez-Herrero and F. Zamora , *Nanoscale*, 2011, **3** , 20 —30

[14] Xiaoyong Chen, Yaoyu Zhao, Longzhi Li, Yuhang Wang, Jiale Wang, Jijun Xiong, Shuanli Du, Ping Zhang, Xiaorong Shi & Jinhong Yu (2020) MXene/Polymer Nanocomposites: Preparation, Properties, and Applications, *Polymer Reviews*, DOI: 10.1080/15583724.2020.1729179

[15] Michael Naguib, Olha Mashtalir, Joshua Carle, Volker Presser, Jun Lu, Lars Hultman, Yury Gogotsi, and Michel W. Barsoum
ACS Nano **2012** *6* (2), 1322-1331
DOI: 10.1021/nn204153h

[16] Naguib, M., Kurtoglu, M., Presser, V., Lu, J., Niu, J., Heon, M., Hultman, L., Gogotsi, Y. and Barsoum, M.W. (2011), Two-Dimensional Nanocrystals Produced by Exfoliation of Ti_3AlC_2. *Adv. Mater*., 23: 4248-4253. doi:10.1002/adma.201102306[17] Mashtalir, O., Lukatskaya, M.R., Zhao, M.-Q., Barsoum, M.W. and Gogotsi, Y. (2015), Amine-Assisted Delamination of Nb_2C MXene for Li-Ion Energy Storage Devices. Adv. Mater., 27: 3501-3506. doi:10.1002/adma.201500604

[18] Seh, Z. W., Fredrickson, K. D., Anasori, B., Kibsgaard, J., Strickler, A. L., Lukatskaya, M. R., Vojvodic, A. (2016). Two-Dimensional Molybdenum Carbide (MXene) as an Efficient Electrocatalyst for Hydrogen Evolution. *ACS Energy Letters*, *1*(3), 589-594. https://doi.org/10.1021/acsenergylett.6b00247

[19] Martin Ade and Harald Hillebrecht
Inorganic Chemistry **2015** *54* (13), 6122-6135
DOI: 10.1021/acs.inorgchem.5b00049

[20] Jeitschko, W. (1969), The crystal structure of Fe_2AlB_2. *Acta Cryst. B*, 25: 163-165. doi:10.1107/S0567740869001944

[21] Babak Anasori, Yu Xie, Majid Beidaghi, Jun Lu, Brian C. Hosler, Lars Hultman, Paul R. C. Kent, Yury Gogotsi, and Michel W. Barsoum
ACS Nano **2015** *9* (10), 9507-9516
DOI: 10.1021/acsnano.5b03591

[22] Okada, S. Synthesis, Crystal Structure and Characterizations of the Ternary Borides TMAlB (TM=Mo,W) with UBC Type Structure. *Trans. Kokushikan Univ. Fac. Eng.* 7–12 (1998).

[23] Toby, B. H., & Von Dreele, R. B. (2013). "GSAS-II: the genesis of a modern open-source all purpose crystallography software package". *Journal of Applied Crystallography*, **46**(2), 544-549.

[24] Kota, S., Zapata-Solvas, E., Ly, A. *et al.* Synthesis and Characterization of an Alumina Forming Nanolaminated Boride: MoAlB. *Sci Rep* **6,** 26475 (2016). https://doi.org/10.1038/srep26475

[25] Lucas T. Alameda, Cameron F. Holder, Julie L. Fenton, and Raymond E. Schaak
Chemistry of Materials **2017** *29* (21), 8953-8957
DOI: 10.1021/acs.chemmater.7b02511

[26] Lucas T. Alameda, Parivash Moradifar, Zachary P. Metzger, Nasim Alem, and Raymond E. Schaak, *Journal of the American Chemical Society* **2018** *140* (28), 8833-8840, DOI: 10.1021/jacs.8b04705

[27] I Ozdemir *et. al.* 2019 *J. Phys.: Condens. Matter* **31** 505401

[28] Lucas T. Alameda, Robert W. Lord, Jordan A. Barr, Parivash Moradifar, Zachary P. Metzger, Benjamin C. Steimle, Cameron F. Holder, Nasim Alem, Susan B. Sinnott, and Raymond E. Schaak
Journal of the American Chemical Society **2019** *141* (27), 10852-10861
DOI: 10.1021/jacs.9b04726

ACADEMIC VITA
Zachary P. Metzger

EDUCATION

The Pennsylvania State University **Class of May 2020**
The College of Engineering | Bachelor of Science in Chemical Engineering
The Schreyer Honors College | Honors in Chemistry

PUBLICATIONS

Publications:

- Lucas T. Alameda, Robert W. Lord, Jordan A. Barr, Parivash Moradifar, Zachary P. Metzger, Benjamin C. Steimle, Cameron F. Holder, Nasim Alem, Susan B. Sinnott, and Raymond E. Schaak. *Journal of the American Chemical Society* **2019** *141* (27), 10852-10861. DOI: 10.1021/jacs.9b04726
- Lucas T. Alameda, Parivash Moradifar, Zachary P. Metzger, Nasim Alem, and Raymond E. Schaak. *Journal of the American Chemical Society* **2018** *140* (28), 8833-8840 DOI: 10.1021/jacs.8b04705

PROFESSIONAL EXPERIENCE

Mondelez International **May 2019-Aug 2019**
Research, Development, and Quality Intern – Global Research East Hanover, NJ

- Identified relationships between product microstructure and performance to help improve product quality
- Overcame complete project restructuring by creating alternative quantitative methods to gather impactful data
- Characterized critical properties of a product to gain an understanding of the root cause of consumer concerns
- Leveraged multiple cross-functional leader's expertise to achieve the deliverables of my summer project

Kimberly-Clark **Aug 2018-Dec 2018**
Global Research & Engineering Co-op - Polymer Science Team Neenah, WI

- Pioneered innovative technology within Kimberly-Clark to solve fundamental product performance issues
- Formulated new product line by applying a material's intrinsic properties in an underdeveloped medium
- Designed new protocol to test for chemical levels in proprietary technology to confidently label safe for use
- Scaled benchtop methods to 500kg amounts to begin production of full products for quality testing

NSF Chemistry Research Experience for Undergraduates (REU) **May 2018-Aug 2018**
Undergraduate Researcher University Park, PA

- Discovered new process to synthesize desired material that reduced post-processing time by 88%
- Obtained the ability to operate independently in an engaged laboratory environment
- Learned sustainability principles to lessen chemical waste and optimize material usage

The Pennsylvania State University **Jan 2017-May 2018**
Chemistry and Chemical Engineering Grader and Proctor University Park, PA

- Collaborated with other proctors to preserve the integrity of the testing environment
- Efficiently answered inquiries regarding examination questions, layout, and correctness
- Followed professors' procedures to ensure that all exams were graded accurately through a homogeneous rubric

LEADERSHIP EXPERIENCE

Vice President for the American Institute of Chemical Engineers (AIChE), *officer since 2017* **Mar 2019-Present**

- Managed 300+ participants during 2019 Chem-E Car event as the key point of contact for all technical and logistical questions
- Aligned students, professors, and volunteers towards a common goal of making the Chem-E Car event successful
- Streamlined communication between university contacts and club officers to facilitate the distribution and usage of chemicals

Engineering Ambassador (EA) **Mar 2018-Present**

- Inspired K-12 students to learn about STEM topics through interactive demos that expose them to a developing field
- Represented Penn State as a proud tour guide to groups of 30+ people providing personal anecdotes for perspective
- Sharpened communication skills by learning a new technical communication style that helps to simplify detailed topics

Chemistry Learning Assistant **Jan 2017-May 2017**

- Acted as a peer liaison in class discussions to mitigate student concerns during open forum sessions
- Assisted students by creating tailored study materials to enhance learning
- Organized weekly review sessions to help students comprehend lecture topics